Particle Size Distribution and Molecular Size Distribution of Polymers in Soap-Free Emulsion Polymerization of Styrene

WEN-YEN CHIU, SUN-MOU LAI, LEO-WANG CHEN, and CHAO-CHENG CHEN

Graduate Institute of Materials Engineering, National Taiwan University, Taipei, Taiwan, Republic of China

SYNOPSIS

Polystrene (PS) particles, generated from soap-free emulsion polymerization of styrene monomer, water, and potassium persulfate, were investigated by photon correlation spectroscopy (PCS) and TEM. The particle size distribution (PSD) was quite uniform. From the data of PCS, it could be said that lots of particles flocculated in the final stage of reaction. It was also deduced from the molecular weight distribution (MWD), measured by GPC, that, during the early stage of reaction, molecules with low molecular weight (< 4000) might exist and the particles were perhaps formed through micellar-type nucleation mechanism. When initiator concentration increased, reaction rate increased but weight average molecular weight, tensile modulus, and elongation decreased. The number density of particles was found to be proportional to 0.49 power of initiator concentration. However, monomer concentration did not seem to have any great effect on all of them above.

INTRODUCTION

Conventional emulsion polymerization has the drawbacks of the pollution of emulsifier and the difficult separation due to emulsifier. Therefore, in 1965 Matsumoto and Ochi[1] proposed to do without the emulsifier, and they successfully prepared the polystrene latex with particles of monodisperse size distribution. Vanderhoff and Van Den Hul[2] listed the wide applications of particles with monodisperse size distribution. For examples, these particles could be used as model colloids and calibration standards. However, "low solids" is still the major problem of emulsifier-free production of latexes.

The preparation of monodisperse latex differs from conventional emulsion polymerization. Three methods are possible: (1) soap-free emulsion polymerization, (2) seeded emulsion polymerization, and (3) soap-free emulsion copolymerization with comonomer functioning as the emulsifier. Goodwin et al.[3] pointed out that the first method was the most basic one and could prepare particles with more versatile size ranges than the second method.

There are mainly three nucleation mechanisms for soap-free systems: the homogeneous nucleation mechanism proposed by Fitch,[4] the coagulation of terminated free radicals propounded by Ugelstad and Hansen,[5] and the micellar-type nucleation brought forward by Goodwin et al.[3] Fitch et al.[4,6,7] argued that conventional Smith–Ewart micellar theory was only applicable for systems with monomers not soluble in water, like styrene. In a study of the KPS/styrene/H_2O system, Goodwin et al.[3] and Goodall et al.[8] found that, in the early stage of reaction, the GPC spectrum showed a peak corresponding to molecular weight less than 1000. They identified the nucleation mechanism as the micellar type. Recently Song and Poehlein[9,10] developed a model to simulate particle nucleation of emulsifier-free aqueous-phase polymerization. This model included the homogeneous nucleation mechanism as well as the *in situ* micellization nucleation mechanism. The particle nucleation period can be divided into two stages. The critical chain length decreased during stage 1 due to the increase of oligomer concentration through significant aqueous phase termination of radicals. Particle size increased during stage 2 through coagulation and polymerization.

Suwa et al.[11] discussed the effects of reaction conditions on the number and size of particles in radiation-induced soap-free emulsion polymerization. He pointed out that the polymerization loci was in

Journal of Applied Polymer Science, Vol. 42, 2787–2793 (1991)
 CCC 0021-8995/91/102787-07$04.00

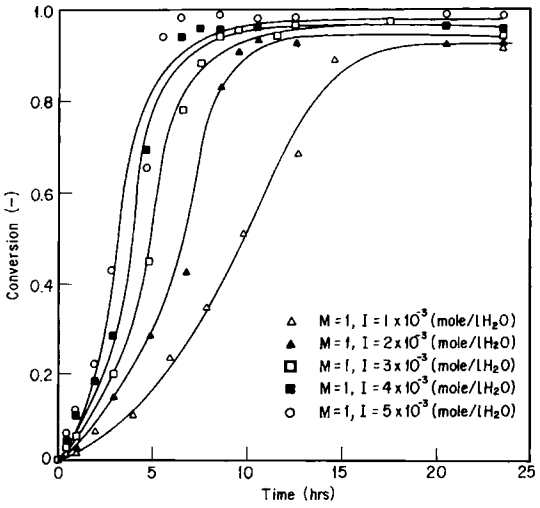

Figure 1 Conversion vs. reaction time.

the water phase. As to the kinetics after the particle formation, Hearn et al.[12] made the point that the bimodal molecular weight distribution could not be explained by conventional theory and that the polymerization possibly proceeded at two sites. Arai et al.[13] compared the polymerization rate of bulk polymerization, emulsion polymerization, and soap-free emulsion polymerization and also studied the effects of mixing rate.[14] In addition, they proposed a kinetic model to discuss the effects of change of monomer and initiator concentrations on particle number for the system MMA/KPS/H_2O.[15]

Due to lack of emulsifier to provide stability, the nucleation mechanism and the time-dependent particle size distribution for soap-free emulsion polymerization is well worth of study. Therefore, in this work, we study the effects of reaction conditions, like monomer and initiator concentration, on the conversion, particle number, molecular weight, mechanical properties, PSD, and MWD. The particle size is probed with photon correlation spectroscopy and TEM.

EXPERIMENTAL

Materials

Styrene monomer was distilled from industrial-grade styrene under a reduced pressure of about 20 mm Hg. Potassium persulfate of reagent grade was used as the initiator.

Emulsion Polymerization

Emulsion polymerization was carried out in a four-neck flask equipped with a two-blade paddle-type impeller, thermometer, nitrogen inlet, and condenser. The polymerization was performed at 70°C with 1–1.5 mol/L H_2O of styrene and 2–5 mmol/L H_2O of KPS. The rate of agitation was kept at 300 ± 25 rpm. Conversion was determined by the gravimetric method of solid product precipitated and dried from the reaction mixture.

Determination of Particle Size and Particle Size Distribution

For TEM and PCS test, 4 mL reaction mixture was taken and diluted with 2 mL hydroquinone aqueous solution. In TEM test, about 15–30 particles were taken to calculate the number average diameter of particles. i.e.,

$$\bar{D}_T = \sum_{i=1} N_i d_i / \sum N_i$$

The information from PCS test could calculate the number average diameter of particles ($\bar{D}_p$) and particle size distribution.

GPC Determination

The MWD and the average molecular weight of polymer were determined by GPC. The pore sizes of four consecutive columns were 100, 500, 10^3, and 10^5 Å. The flow rate for THF was 1 mL/min at 23°C.

Mechanical Properties

The sample taken from the reaction mixture which had reacted for 24 h was hot-pressed and then tested

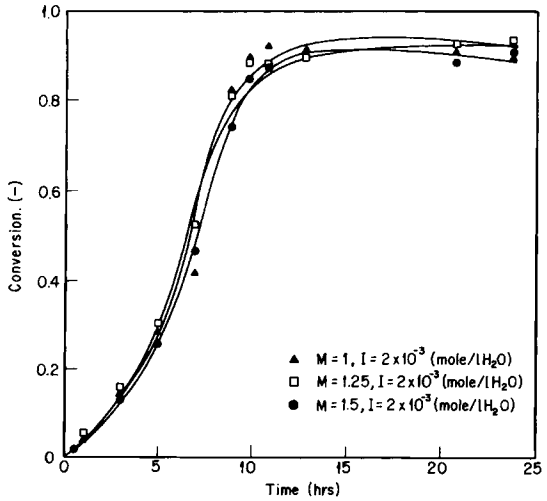

Figure 2 Conversion vs. reaction time.

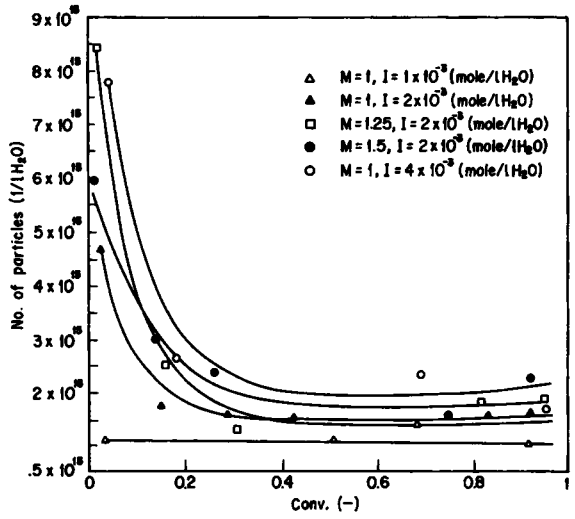

Figure 3 Number of particles (1/L H_2O) vs. conversion.

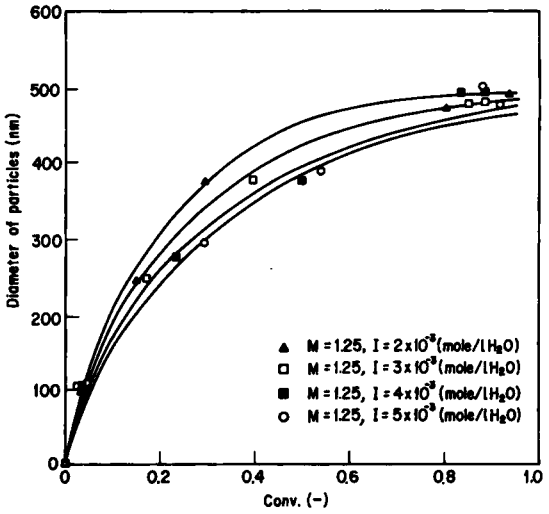

Figure 5 Number average diameter of particles (TEM) vs. conversion.

by Instron machine at 23°C according to ASTM-1708-79 with 10 mm/min of strain rate. The modulus, tensile strength, and elongation were determined.

RESULTS AND DISCUSSION

Conversion

Figures 1 and 2 show plots of conversion against time. It can be seen that the initiator can enhance the reaction rate. But the increase in monomer concentration does not have much effect on reaction rate. This is possibly because more particles are generated by increasing initiator concentration, but this effect is not evident for raising monomer concentration. Similar results were reported in Song and Poehlein's work.[16]

Particle Number

From Figure 3, we can find that the number of particles decreases with time and finally reaches a steady value. We suppose that this phenomenon is due to the coagulation of particles. In the early period of reaction, primary particles are formed possibly through micellar-type nucleation. Since these primary particles are swollen in monomer and soft, they

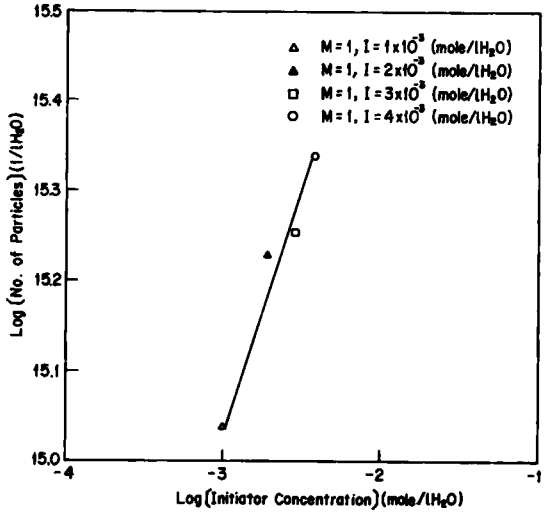

Figure 4 Number of particles (1/L H_2O) vs. initiator concentration.

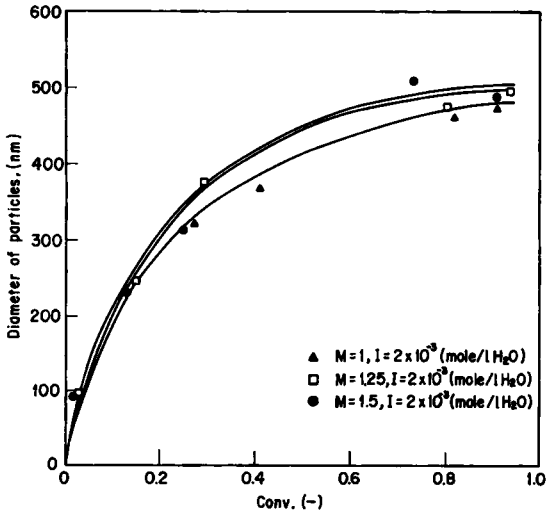

Figure 6 Number average diameter of particles (TEM) vs. conversion.

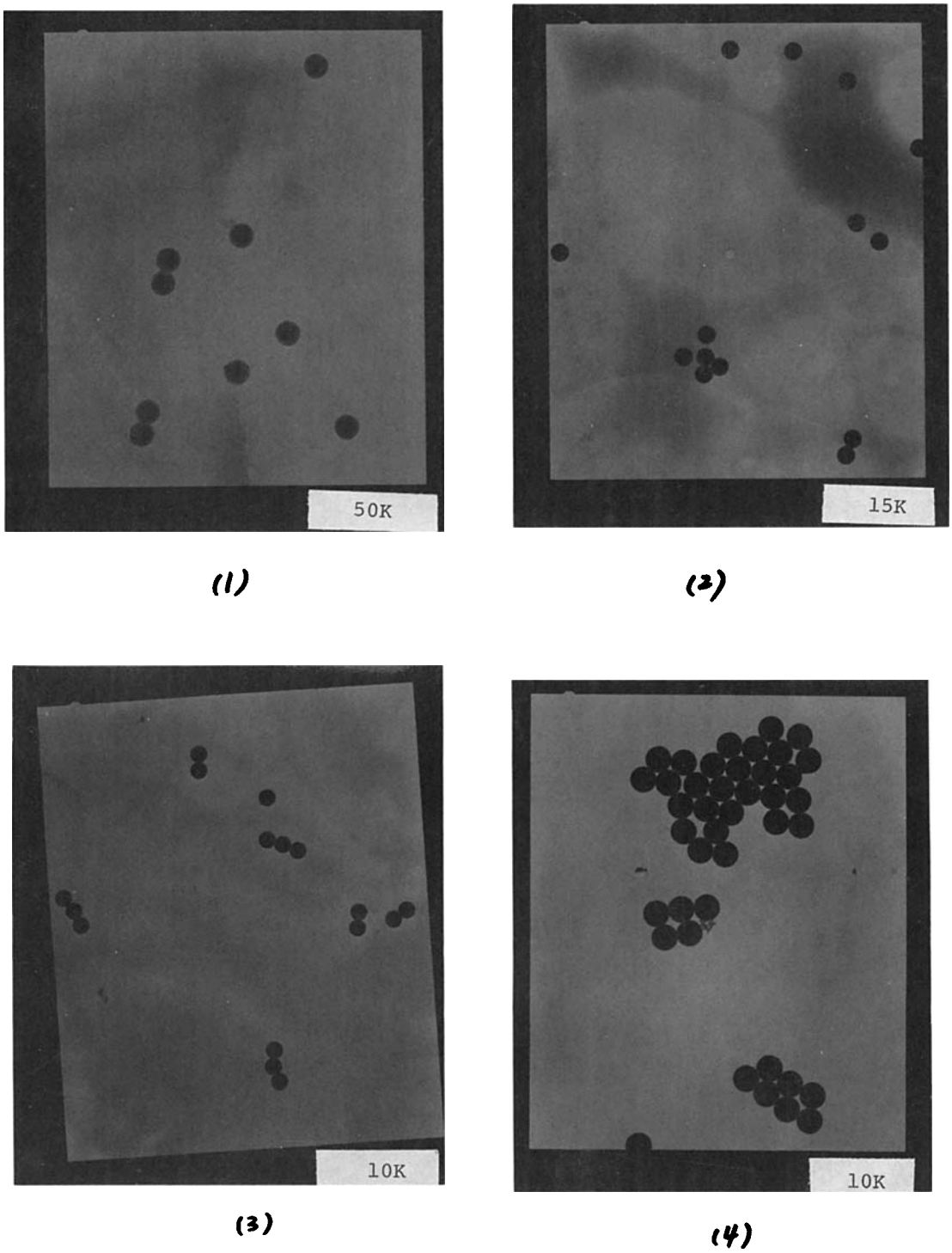

Figure 7 TEM pictures of polymer particles at different reaction times in soap-free emulsion polymerization with $M = 1.5$, $I = 2.0 \times 10^{-3}$ (mol/L H_2O): (1) $t = 30$ min, $\bar{D}_T = 92.4$ nm; (2) $t = 3$ h, $\bar{D}_T = 231.9$ nm; (3) $t = 5$ h, $\bar{D}_T = 314.6$ nm; (4) $t = 24$ h, $\bar{D}_T = 489.8$ nm.

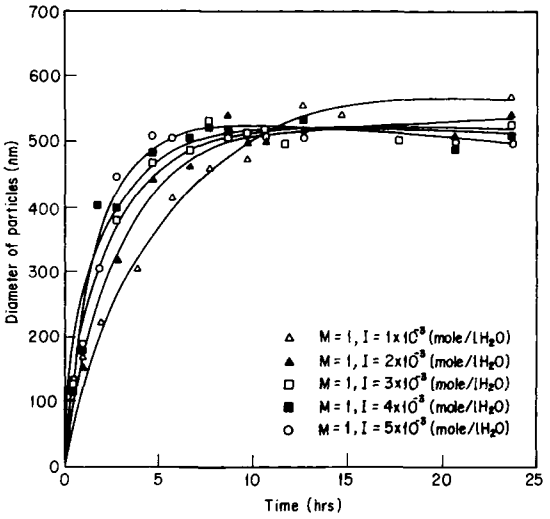

Figure 8 Number average diameter of particles (PCS) vs. reaction time.

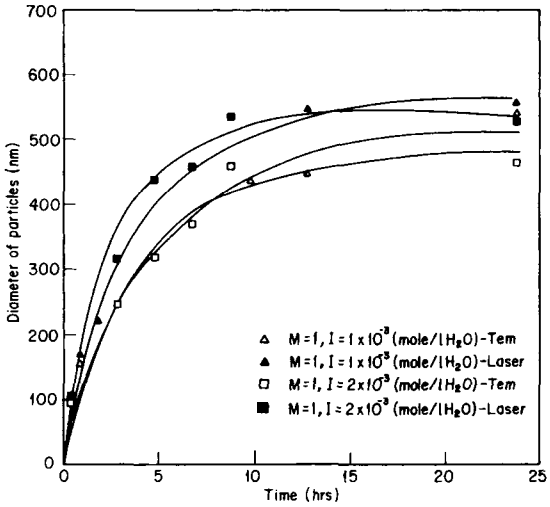

Figure 9 Number average diameter of particles (TEM and PCS) vs. reaction time.

can floculate together if collisions take place. Besides, once the surface charge density can no longer maintain the stability after the particles growing, particles coagulate to reestablish stability. Therefore, the particle number is first decreased by coagulation of particles. However, in the latter period of reaction, the coagulation is less likely to happen because the monomer is being run out and particles are hardened. This is why the number of particles finally stays unchanged. In the mean time, the particle sizes tend to be uniform for the reason of the so-called competitive growth, which means small particles grow faster than large particles by way of limited coagulation. Figure 3 also shows that particle number increases with initiator concentration but not affected by monomer concentration. In Figure 4 the particle number is shown to increase linearly with the 0.49 power of initiator concentration.

Particle Size

Figures 5 and 6 plot particle size obtained from TEM as a function of conversion. The particle size distribution was quite sharp from the TEM observation (Fig. 7). These figures show that small particles are obtained with higher initiator concentration or with lower monomer concentration. The similar phenomena were found in Song and Poehlein's work too.[16] This could be explained by the effect of initiator and monomer concentration on particle number mentioned above. Figure 8 are the results of how average particle size changes with time obtained from the PCS. The particle size gradually approaches a constant when monomer is being used up. Figure 9 compares the results from TEM and PCS. The values taken from PCS are greater than those of TEM. This is because of the swelling effect of monomer in the early stage of reaction and the second peak found on PCS spectrum in the latter stage, both of which cause $\bar{D}_p$ (from PCS) larger than $\bar{D}_I$ (from TEM).

Particle Size Distribution

Figure 10 shows the particle size distribution obtained from PCS versus reaction time. A small sec-

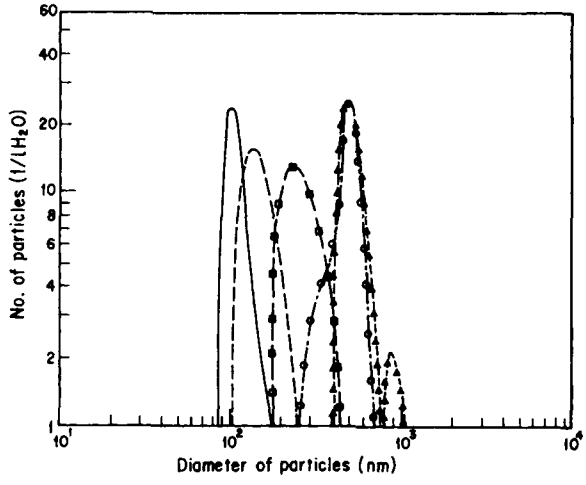

Figure 10 Particle size distribution, $M = 1.5$, $I = 2 \times 10^{-3}$ (mol/L H_2O): (——) $t = 30$ min; (---) $t = 1$ h; (□□) $t = 3$ h; (○○○) $t = 5$ h; (△△) $t = 24$ h.

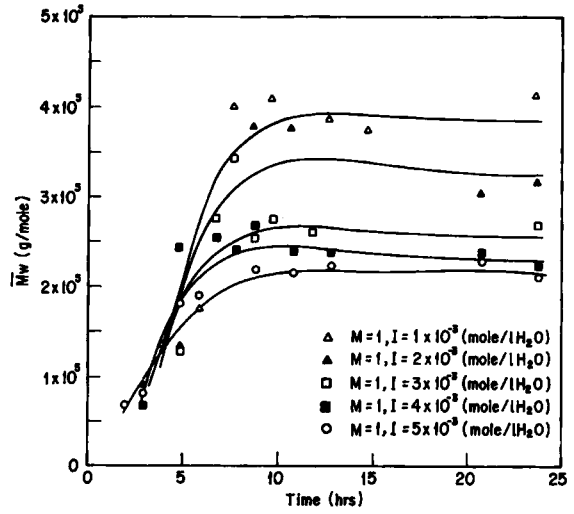

Figure 11 Weight average molecular weight of polymer vs. reaction time.

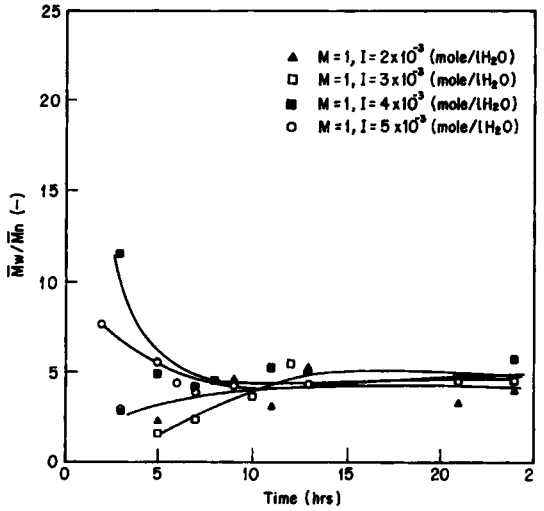

Figure 13 Polydispersity of polymer vs. reaction time.

ond peak appears at about 760.9–837.5 nm in the later period of reaction, which might indicate bimodal size distribution. It is noteworthy that the second peak in Figure 10 appears at about the position which represents particles twice the diameter as those at the first peak. There could be two possibilities. One is that the second peak is truly caused by large particles. The other is that the peak actually represents a floc of two particles. However, what we see under TEM is uniform particles only. Therefore, we are assured that floculation occurs during latter stage of reaction. Again, it explains why $\bar{D}_p$ is larger than $\bar{D}_T$, as mentioned above.

Average Molecular Weight

In Figures 11 and 12, the weight average molecular weight ($\bar{M}_w$) is plotted as a function of time. As reaction proceeds, the $\bar{M}_w$ first increases to a maximum and then decreases to a constant. $\bar{M}_w$ is lowered by raising initiator concentration because monomer is thus divided among more particles. It is also found that the effect of monomer concentration on $\bar{M}_w$ is not evident. The polydispersity ($\bar{M}_w/\bar{M}_n$) obtained from the data above is shown against time in Figures 13 and 14. Neither do these figures show any common relations among them, except that $\bar{M}_w/\bar{M}_n$ first undergoes significant change with time but later the rate of change moderates.

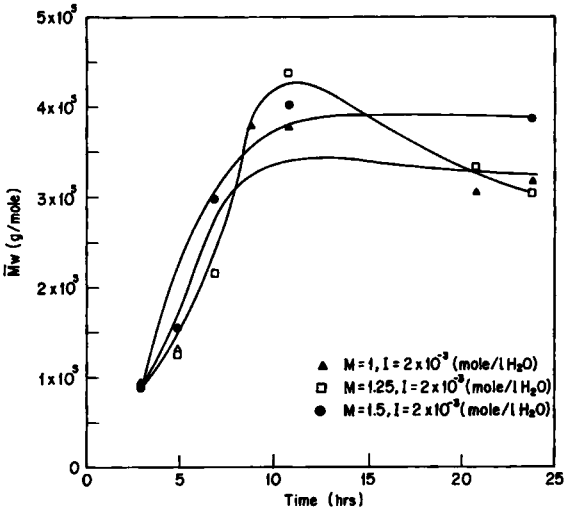

Figure 12 Weight average molecular weight of polymer vs. reaction time.

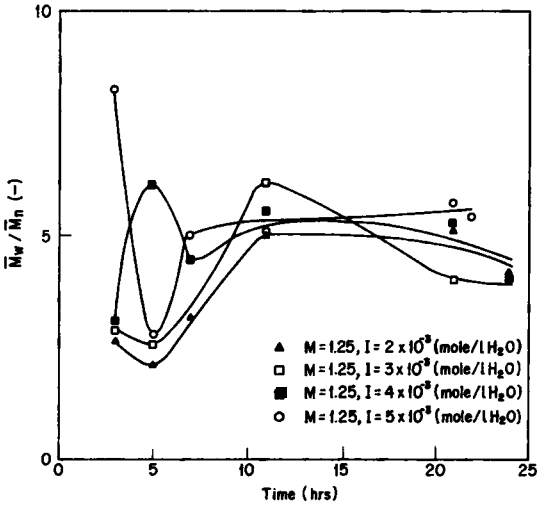

Figure 14 Polydispersity of polymer vs. reaction time.

Molecular Weight Distribution

The way the molecular weight distribution (MWD) changes with time can be seen in Figure 15. The results first show a binodal distribution with the peak of low molecular weight at about 4000 (data taken at a reaction time of 30 min). This peak moves toward higher molecular weight for samples taken at longer reaction time. Finally, a monodispense distribution is observed. The phenomenon that many molecules of low molecular weight exist in early stage of reaction was also mentioned by Goodwin et al.[3] and Goodall et al.[18] and inspired them to bring forward their micellar type nucleation. Besides, after comparing PSD and MWD, we conclude that no quantitative relations could be established between them. It is for the reason that in the early stage the PSD is monodisperse and the MWD is bimodal, but in the latter stage the case is reversed. But, whichever distribution curve the MWD is, the particles are seen to be uniform under TEM.

Mechanical Properties

Figure 16 shows the effect of initiator concentration on tensile modulus, tensile strength, and elongation. We mentioned in the section of Average Molecular Weight above that higher initiator concentration lowered the $\bar{M}_w$. Therefore, the differences in mechanical properties probably come from the molecular weight differences. It is reasonable that polystyrene with higher molecular weight would exhibit higher modulus, higher tensile strength, and higher toughness (or elongation).

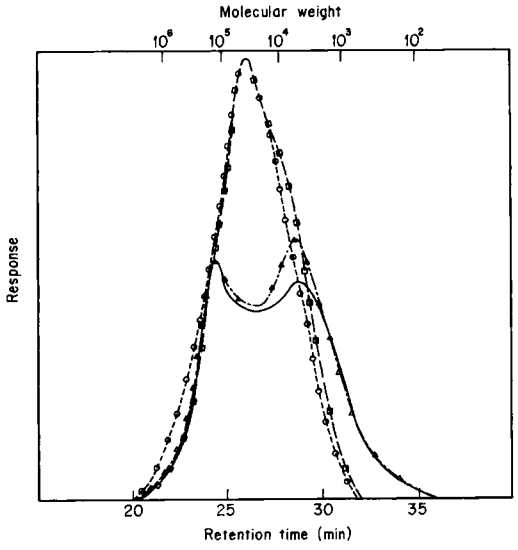

Figure 15 Molecular weight distribution of polymer, M = 1, $I = 5 \times 10^{-3}$ (mol/L H_2O) (——) t = 30 min; (△△) t = 1 h; (□□) t = 2 h; (○○○) t = 24 h.

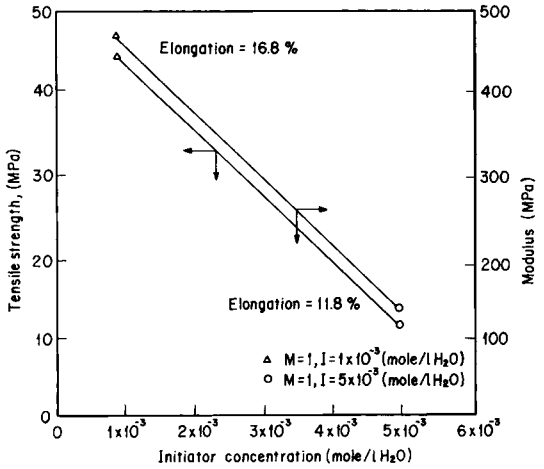

Figure 16 Effect of initiator concentration on mechanical property of polymer.

REFERENCES

1. T. Matsumoto and A. Ochi, *Kobunshi Kagaku,* **22,** 481 (1965).
2. J. W. Vanderhoff and H. J. Van Den Hul, *J. Macromol. Sci. Chem.,* **A7**(3), 677 (1973).
3. J. W. Goodwin, J. Mearn, C. C. Ho, and R. H. Ottewill, *Br. Polym. J.,* **5,** 347 (1973).
4. R. M. Fitch, *Br. Polym. J.,* **5,** 467 (1973).
5. J. Ugelstad and F. K. Hansen, *Rubber Chem. Technol.,* **49,** 536 (1976).
6. R. M. Fitch, *Polym. Lett.,* **8,** 703 (1970).
7. R. Watson, R. M. Fitch, and D. Bakker, *Polym. Prepr.,* **16,** 109 (1975).
8. A. R. Goodall, M. C. Wilkinson, and J. Hearn, *J. Polym. Sci. Polym. Chem. Ed.,* **15,** 2193 (1977).
9. Z. Song and G. W. Poehlein, *J. Colloid Interface Sci.,* **128**(2), 501 (1989).
10. Z. Song and G. W. Poehlein, *J. Colloid Interface Sci.,* **128**(2), 486 (1989).
11. Takeshi Suwa, Terutaka Watanabe, Tadao Seguchi, Jiro Okamoto, and Sueo Machi, *J. Polym. Sci. Polym. Chem. Ed.,* **17,** 111 (1979).
12. J. Hearn, M. C. Wilkinson, A. R. Goodall, and M. Chaine, *J. Polym. Sci. Polym. Chem. Ed.,* **23,** 1869 (1985).
13. M. Arai, K. Arai, and S. Saito, *J. Polym. Sci. Polym. Chem. Ed.,* **18,** 2811 (1980).
14. K. Arai, M. Arai, S. Iwasaki, and S. Saito, *J. Polym. Sci. Polym. Chem. Ed.,* **19,** 1203 (1981).
15. M. Arai, K. Arai, and S. Saito, *J. Polym. Sci. Polym. Chem. Ed.,* **17,** 3655 (1979).
16. Z. Song and G. W. Poehlein, Thesis report, School of Chemical Engineering, Georgia Institute of Technology, Atlanta, 1989.

Received April 9, 1990
Accepted September 6, 1990